

Complexity Analysis of Heuristic Pulse Interleaving Algorithms for Multi-Target Tracking with Multiple Simultaneous Receive Beams

Dae-Sung Jang and Han-Lim Choi*

Abstract

This paper presents heuristic pulse interleaving algorithms for multi-target tracking on pulse Doppler phased array radars that can process multiple simultaneous received beams. The pulse interleaving problems for element and subarray level digital beamforming architectures are formulated as the same integer program and the asymptotic time complexities of the algorithms are analyzed.

Index Terms

Pulse Interleaving, Pulse Doppler Phased Array Radar, Multiple Simultaneous Receive Beams, Digital Beamforming

I. INTRODUCTION

In target detection of a radar, round-trip electromagnetic wave propagation between a radar and a target forms an intervening idle time between a transmitted pulse (T-pulse) and a received pulse (R-pulse). The use of the intervening idle time can reduce the time for track and search and thus enhances resource utilization and overall performance of a radar. A technique that inserts T/R-pulses in the idle time of other pulses is called pulse interleaving. The pulse interleaving technique utilizes hidden resources of a radar, i.e. unused times so that, for example, the pulse interleaving of tracking tasks reduces the total tracking time and the resultant saved time can be used for tracking additional targets or enhancing the search performance.

There are two types of pulse interleaving: task-level interleaving and pulse-level interleaving. In task-level interleaving, a radar task, which may consist of several looks or a look with a number of pulses is the unit of interleaving. Transmitted and received dwells of a task are interleaved with the dwells of

D.S. Jang and H.-L. Choi are with the Division of Aerospace Engineering, KAIST, Daejeon, 305-701, Republic of Korea. E-mail: (dsjang@lics.kaist.ac.kr, hanlimc@kaist.ac.kr).

*All correspondence should be forwarded to H.-L. Choi; Mailing address: 291 Daehak-ro, Rm. E4-C327, C-FRIEND Field Robotics Center, KAIST, Yuseong, Daejeon 305-701, Rep. of Korea.; Tel:+82-42-350-3727; E-mail: hanlimc@kaist.ac.kr

other tasks and thus a typical target range is required to be long for a sufficient idle time compared with the dwells. Meanwhile, pulse-level interleaving is available if a group of pulses in a look has sufficient intervening idle times between the pulses. This level of interleaving allows R-pulses to be interleaved not only with the pulses of other looks but with the T-pulses that the R-pulses originate from. Therefore, a longer dwell time of a look can be used for a comparatively shorter target range.

There have been some previous approaches to pulse interleaving of radar tasks [1]–[7], but most of them dealt with task-level interleaving [2]–[6]. The previous studies of task-level pulse interleaving assumed that the lengths of intervening idle times were exactly known or well predicted. Minimizing the maximum completion time of tasks is a NP-hard problem even in this case [8]–[10], and thus heuristic algorithms [8] and approximation algorithms [6], [10] were presented for the problem. In pulse-level interleaving, additional considerations are required on radar system capabilities and interleaving constraints brought by signal processing requirements, which hinder any extensions from the studies of task-level interleaving.

The task-level interleaving in a multi-function phased array radar is usually formed as a coupled-task scheduling [2]. The coupled-task scheduling is a problem that decides on the time and the order of performing the tasks, where each coupled-task consists of a pair of T/R-pulses and an intervening idle time, which allows task scheduler to interleave other coupled-tasks into it. Pulse interleaving enhances utilization of a radar by reducing unused times, whereas the radar consumes more energy and produces more heat. Therefore, some constraints that reflect limitations of energy resources and heat generation were considered in the pulse interleaving of coupled-tasks [3]–[5]. In [3], an energy constraint was considered in real-time template based coupled-task scheduling. A concept of schedulability envelope was used in [4] to provide a quantitative abstraction for a schedulability check under duty cycle and energy constraints, and multiple target tracking was controlled by an on-line scheduler with the schedulability envelope to enhance radar system utilization while satisfying the constraints. In [5], radar power constraints were considered in near-optimal resource allocation by a quality of service (QoS) optimization and the scheduling of coupled-tasks.

The results of task-level interleaving have not been extended to pulse-level interleaving, since pulse repetition in a look, which restricts the feasibility of pulse interleaving, needs to be considered in pulse-level interleaving. In pulse-level interleaving, usually applied to pulse Doppler radars, the pulses are repeated with a specified frequency by requirements for signal processing. The frequency of these pulses is called a pulse repetition frequency (PRF) and its inverse is a pulse repetition interval (PRI). The PRF/PRI can be different among tasks since available PRFs for target detection are dependent on eclipsing, clutter conditions, and the range and radial velocity of the target. Therefore, PRF selection of interleaved looks in pulse-level interleaving is a significant factor since looks of different PRFs can not be mutually interleaved

to prevent overlapping in the time axis. This makes direct applications of the previous task-level works to pulse-level interleaving difficult without any consideration on the pulse Doppler scheme.

In pulse-level interleaving under the pulse Doppler scheme, a radar has to alternate waveforms and beam directions from pulse to pulse at every PRI. A phased array radar (PAR) system enables this pulse-to-pulse alteration by rapid electronic beam steering. The pulse interleaving problem in a pulse Doppler PAR was firstly considered in [1] for multiple target tracking and a heuristic algorithm was presented to reduce the tracking time of the targets. Several heuristic rules were also studied in [7] with energy constraints and priorities of tasks, and all the tasks were assumed to use the same PRF. However, in both studies, it was not mentioned how to determine the PRFs of interleaved looks from different targets, each of which has different available PRFs.

In [1], [7], it was assumed that R-pulses as well as T-pulses must not be overlapped each other since signals from different directions can not be separated without an appropriate beamforming technique. A digital beamforming (DBF) technique of a PAR can identify the signals from different directions and enhance interleaving possibilities by relieving one of the constraints of interleaving pulses. By DBF, a receive beam can be digitally re-steered and processed to form multiple simultaneous receive beams [11], which means a received signal from a wide beam is processed as multiple signals from different directions at the same time. For search, multiple simultaneous receive beams (MSRB) bring a reduction of search frame time [11], [12]. Also, for pulse interleaving in multiple target tracking, the MSRB technique allows R-pulses to be overlapped each other, thus the facilitated pulse interleaving reduces overall track occupancy more. The surplus radar time by reduced track occupancy can be utilized for tracking more targets or distributing to other radar functions to enhance their performance.

The contribution of this paper is threefold. First, pulse-level interleaving using MSRB by digital re-steering is considered for multiple target tracking in a pulse Doppler PAR. DBF is implemented in element or subarray level; since element level DBF (EDBF) is limited practically, most of PARs in service are developed to have subarray level DBF (SDBF). The interleaving problem using MSRB is formulated by an integer program valid for two different levels of DBF architecture. Second, this paper also includes considerations of PRF selection for the pulse interleaving in both DBF levels and a geometric constraint of MSRB in SDBF. In EDBF, a received beam can be re-steered in an arbitrary direction, whereas the re-steering direction is limited in SDBF. Therefore, the pulse interleaving using MSRB in SDBF has, additionally, a selection problem of targets that will be tracked by a group of interleaved looks within the region of the re-steerable direction. Third, heuristic pulse interleaving algorithms are presented as practical solutions for both problems of the two DBF levels, and the complexity analysis of the algorithms is carried out.

The rest of this paper is organized as follows. Section II describes physical constraints and properties of the pulse interleaving in a pulse Doppler PAR with MSRB of the two different DBF levels. In section III, the pulse interleaving problems of the two DBF levels for multiple target tracking are formulated. In section IV, the heuristic interleaving algorithms are presented and the complexity analysis of the algorithms is demonstrated in section V. Section VI provides the summary of the paper and concluding remarks.

II. BACKGROUND OF PULSE INTERLEAVING

A. Pulse Interleaving in Pulse Doppler Radar

In pulse Doppler radars, a number of pulses in a look are transmitted with a certain PRF to acquire target's radial velocity by measuring a Doppler shift of a received signal. A look is a group of pulses repeated with a certain PRF and it can be regarded as a unit of creating a measurement of a target. For airborne case, a look with a high PRF can measure the Doppler shift unambiguously, but range measurements are highly folded [13]. Conversely, a low PRF has good range unambiguity and can reduce sidelobe detection by sensitivity time control, whereas it has poor ground moving target rejection and Doppler ambiguity [11], [13], [14]. A medium PRF, usually 10-40kHz, has both range and Doppler ambiguity, but it shows a compromise of performance at all aspect target detection under the presence of clutter [11], [15], [16].

The range and radial velocity of a target are measurable without ambiguity if the range and Doppler shift are smaller than an unambiguous range R_u and an unambiguous frequency f_u , respectively:

$$R_u = \frac{ct_r}{2} = \frac{c}{2f_r}, \quad f_u = f_r \quad (1)$$

where c is speed of light, t_r is PRI, and f_r is PRF. The received signal from the target is folded when its actual target range is greater than R_u or the Doppler frequency is larger than f_u . An ambiguous range R_a and an ambiguous frequency f_a are measurable quantities from the folded received signal:

$$R_a \equiv R \mod \frac{c}{2f_r} \quad (2)$$

$$f_a \equiv \frac{-2V_t}{\lambda} \equiv f_s \mod f_r \quad (3)$$

where R is the range between the target and a radar, V_t is the target's radial velocity with respect to the ground, λ is the wave length of the radar, and f_s is defined as the Doppler shift of the received signal.

In a search beam, multiple PRFs are used to solve the range and Doppler ambiguities since the radar system has no prior information of a detected target. However, a track beam can be formed by single-PRF looks using the target's range/velocity estimate and covariance from a tracking filter. Thus, in this paper,

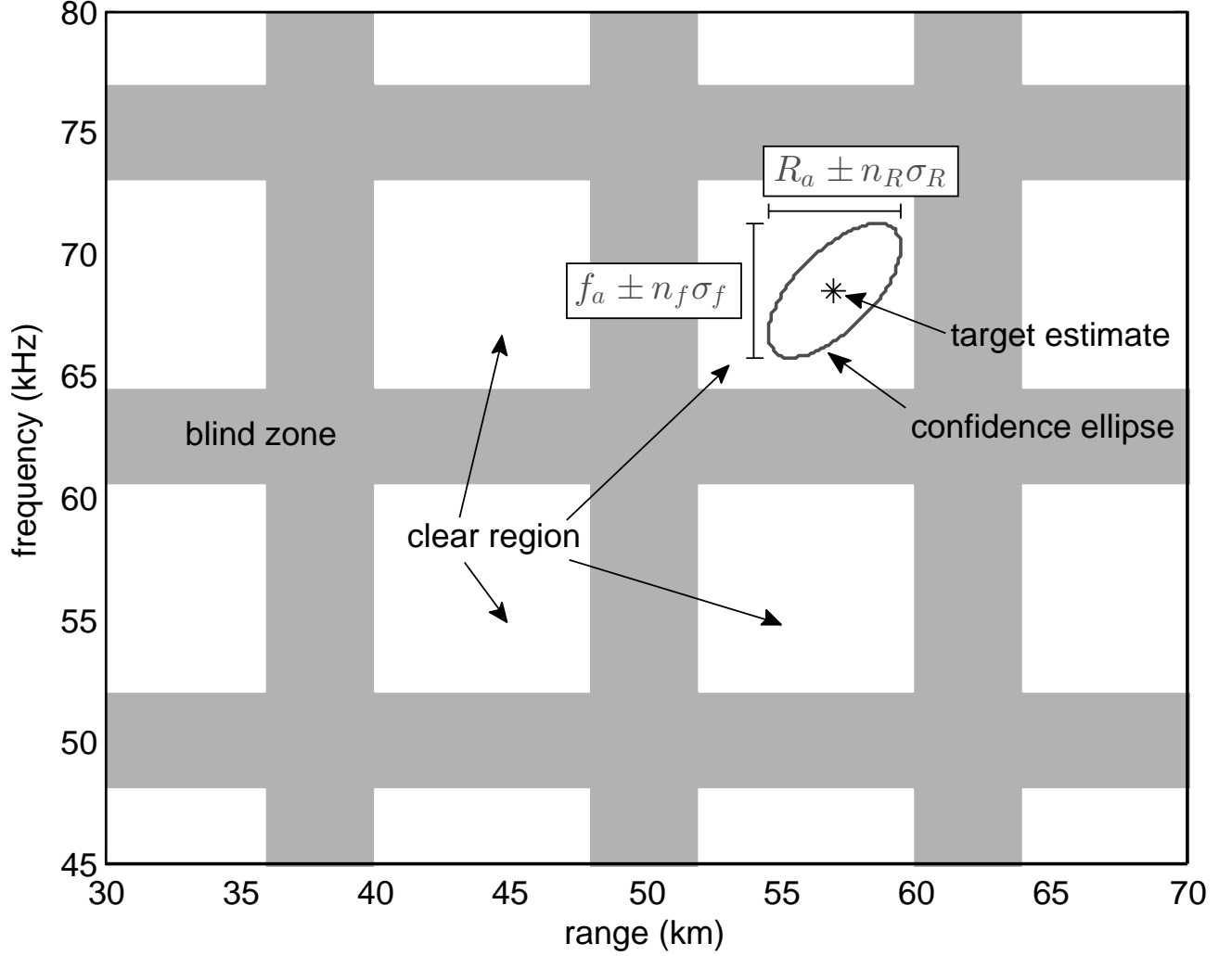


Fig. 1. The blind zones (gray) and clear regions (white) of target tracking by $f_r=12.5\text{kHz}$. The ellipse depicts a boundary specified by multiples of standard deviations for the estimate(*).

a tracking task of a target uses a single PRF at each time, selected among a predesigned set of PRFs.

Target detection is greatly restricted in blind zones induced from the losses by pulse eclipsing and clutter in the range and frequency domain of interest. In this paper, it is assumed that the blind zones are placed around the folded frequencies and ranges that are the integer multiples of f_u and R_u , respectively. This can be appropriate when a rejection notch is at main beam clutter and a target's radial velocity with respect to the ground is measured in a Doppler pass band [11], [15], [17]. Fig. 1 shows the blind zones and the clear regions of $f_r=12.5\text{kHz}$ as a sample of medium PRF. The widths of the blind zones are assumed as 4kHz for frequency and 4km for range. An estimated state of range and radial velocity of a target from a tracking filter is plotted on a clear region in Fig. 1. An ellipse around the estimate is a boundary specified by multiples of standard deviations. If this ellipse is totally within clear region, the target can be detected at the next track update with a high probability.

Under an assumption that the distribution of target's range and frequency (or equivalently radial velocity)

are Gaussian, the confidence intervals of the target range and the Doppler frequency are described as $R_a \pm n_R \sigma_R$ and $f_a \pm n_f \sigma_f$ with appropriately chosen multiples n_R and n_f , where σ_R and σ_f denote standard deviations of the target range and Doppler frequency. Then, if the confidence intervals lie completely within the clear region of a PRF, the target can be detected using the PRF with a probability, at least, according to the sigma multiples n_R, n_f . Therefore, the following conditions need to be satisfied in order to track a target with f_r :

$$\epsilon_R^+ \leq R_a - n_R \sigma_R, \quad R_a + n_R \sigma_R \leq R_u - \epsilon_R^- \quad (4)$$

$$\epsilon_f^+ \leq f_a - n_f \sigma_f, \quad f_a + n_f \sigma_f \leq f_u - \epsilon_f^- \quad (5)$$

where left-end blind widths $\epsilon_R^+, \epsilon_f^+$ and right-end blind widths $\epsilon_R^-, \epsilon_f^-$ are defined below.

$$\epsilon_R^+ = \max \left\{ C_R^+, \frac{ct_p}{2} \right\}, \quad \epsilon_R^- = C_R^- + \frac{ct_p}{2} \quad (6)$$

$$\epsilon_f^+ = C_f^+, \quad \epsilon_f^- = C_f^- \quad (7)$$

$C_R^+, C_R^-, C_f^+, C_f^-, t_p$ are left-/right-end clutter regions along range domain, ones along frequency domain, and the pulse width of a track beam, respectively.

If a target can be tracked with a given PRF and there are enough intervening idle times of T/R-pulse trains in a tracking task of the target, it is possible to interleave the pulse trains of another target's task with the same PRF. However, if the PRFs of two looks are different, it is highly probable that pulses in the looks are overlapped, in particular, when the looks consist of a large number of pulses.

Consider four targets that are to be tracked by a pulse Doppler PAR with three different PRFs: target 1 satisfies (4) and (5) for PRF 1 and 2, and thus it can be tracked with those PRFs; in a similar way, target 2 is trackable with PRF 2 and 3, while target 3 is trackable with PRF 2, and target 4 is trackable with PRF 1 and 3. It is assumed that each target is assigned to a tracking task that consists of several looks with a PRF, and the periods of tracking tasks are similar and requested intervals of execution of tasks are concentrated in a short time. In this case, target 1 and 4 are trackable with PRF 1; target 1, 2, and 3 are trackable with PRF 2; target 2 and 4 are trackable with PRF 3. Fig. 2a describes one example of interleaved pulses in a single PRI when the pulse interleaving of the three tracking tasks is possible with PRF 2. As the figure shows, all T-pulses and possible intervals of R-pulses defined by the range estimates and standard deviations should not intersect with each other at any time points. Also, note T-pulses are delayed by other preceding T-pulses and thus the corresponding R-pulses are also delayed by the same amount of times.

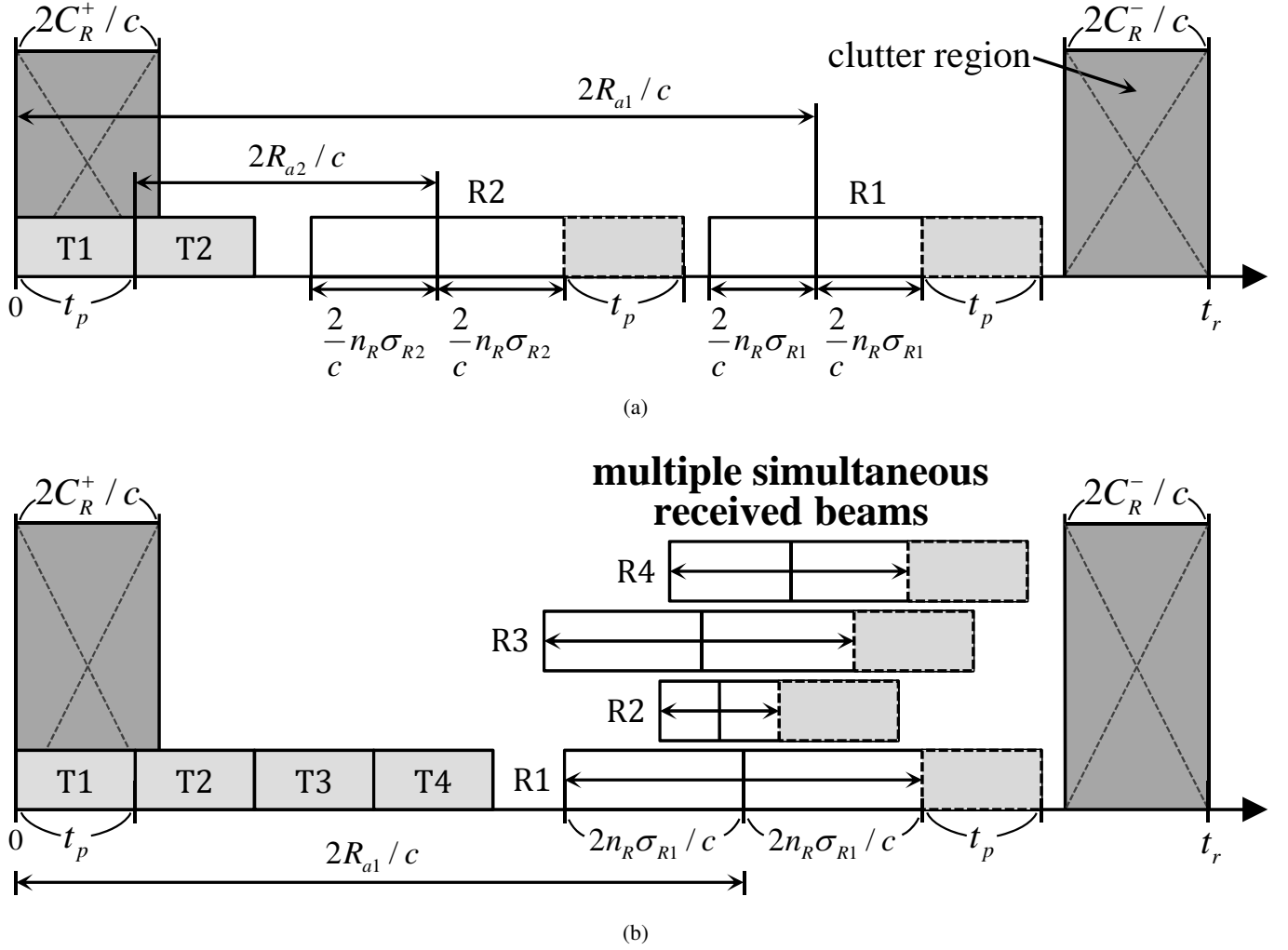


Fig. 2. A pulse interleaving scheme in a single PRI for a pulse Doppler PAR (a) without MSRB and (b) with MSRB. T/R-pulses of tasks are marked with ‘T’ and ‘R’ followed by the task numbers. R_{a1} and σ_{R1} are the range and the standard deviation of the target of task 1, and R_{a2} and σ_{R2} are the ones of task 2.

B. Pulse Interleaving with Multiple Simultaneous Receive Beams

In pulse interleaving for multiple target tracking, the non-overlapping constraint of R-pulses can be relieved by the MSRB technique. The MSRB technique is implemented by digital beamforming and re-steering of a received beam; in multiple target tracking, a radar can handle multi-target returns from different directions even if the pulses are actually received simultaneously. Fig. 2b depicts a pulse interleaving scheme with MSRB in a PRI. It should be noted that, by MSRB, more tasks can be interleaved with the same length of pulses and even longer estimated intervals of R-pulses.

Pulse Doppler PARs using solid state transmit/receive modules typically have lower peak power and a higher duty ratio. Thus, the maximum number of interleaved pulses in a PRI is limited to a small constant with a beam of a high duty ratio. Furthermore, the estimated time intervals of received signals have much longer lengths than T-pulses. Thus, interleaving received signals between T-pulses in a PRI is rarely beneficial, since received signals of different T-pulses can be processed simultaneously. Therefore,

for the sake of simplicity of the interleaving scheme, T-pulses successively positioned from the starting time of each PRI are only considered in this paper (see Fig. 2b). This simplifies the problem while still including most physically feasible cases. Additionally, interleaving of successively attached pulses that satisfy duty ratio is assumed to meet any energy constraint of the radar.

Since interleaved T-pulses of tracking tasks are transmitted separately, any adequate beamforming for individual tracks to different directions is allowed on transmission. On the other hand, the directions of received beams are restricted by re-steering capability of a PAR, where the capability is determined by the type of the DBF architecture. In EDBF, received signals are digitized at each array element whereas a combined received signal at each subarray is digitized in SDBF. The digitized signal is weighted and delayed in a digital beamformer where multiple independent beams can be formed in different directions. The independent beams can be steered into any direction in EDBF [11]. However, SDBF is preferred to be implemented than EDBF on account of practical reasons (e.g. size, cost, and computation). In SDBF, only the array factor of a received beam can be digitally re-steered, but the subarray pattern of the received beam is maintained at an originally steered direction set by phase shifters. Therefore, grating lobes of the array factor escaped from the nulls of the subarray pattern create high sidelobes [18]. This can be attenuated by an overlapped subarray and low sidelobe weighting, but the re-steering direction is limited: the extent is within the subarray pattern [11], [18], [19].

The limitation on re-steering capability of MSRB restricts the interleaving possibility in SDBF by angular distances of multiple targets besides PRF availabilities. The interleaving possibility of targets under the limited re-steering can be discriminated in a plane of direction cosines of beam scanning direction, called T plane in [20]. In this paper, normalized scanning plane denotes the plane of direction cosines since any point on the plane is a normalized projection from a point on a hemisphere where a target can locate. The normalized scanning plane is confined in a unit disk centered at the origin. Fig. 3 depicts projected points of targets trackable with the same PRF and re-steering boundaries of MSRB on the normalized scanning plane. Since trackable targets are different depending on the PRF, a similar figure can be drawn for each PRF. If a circle beam is used and the corresponding subarray pattern is also circular, the re-steerable area of MSRB forms a disk. Some examples of such disks are plotted in Fig. 3: targets within each disk are allowed to try interleaving. Without considering directivity loss and other factors, a disk with more targets is preferred as long as the targets are enclosed by the disk. In Fig. 3, disk A encloses two targets around the origin and disk B encloses another target in addition to the targets, thus it is enough to consider disk B for pulse interleaving. In this way, the limitation of the pulse interleaving using MSRB in SDBF can be identified as this geometric constraint of equal-sized disks covering projected target points on the normalized scanning plane for each PRF.

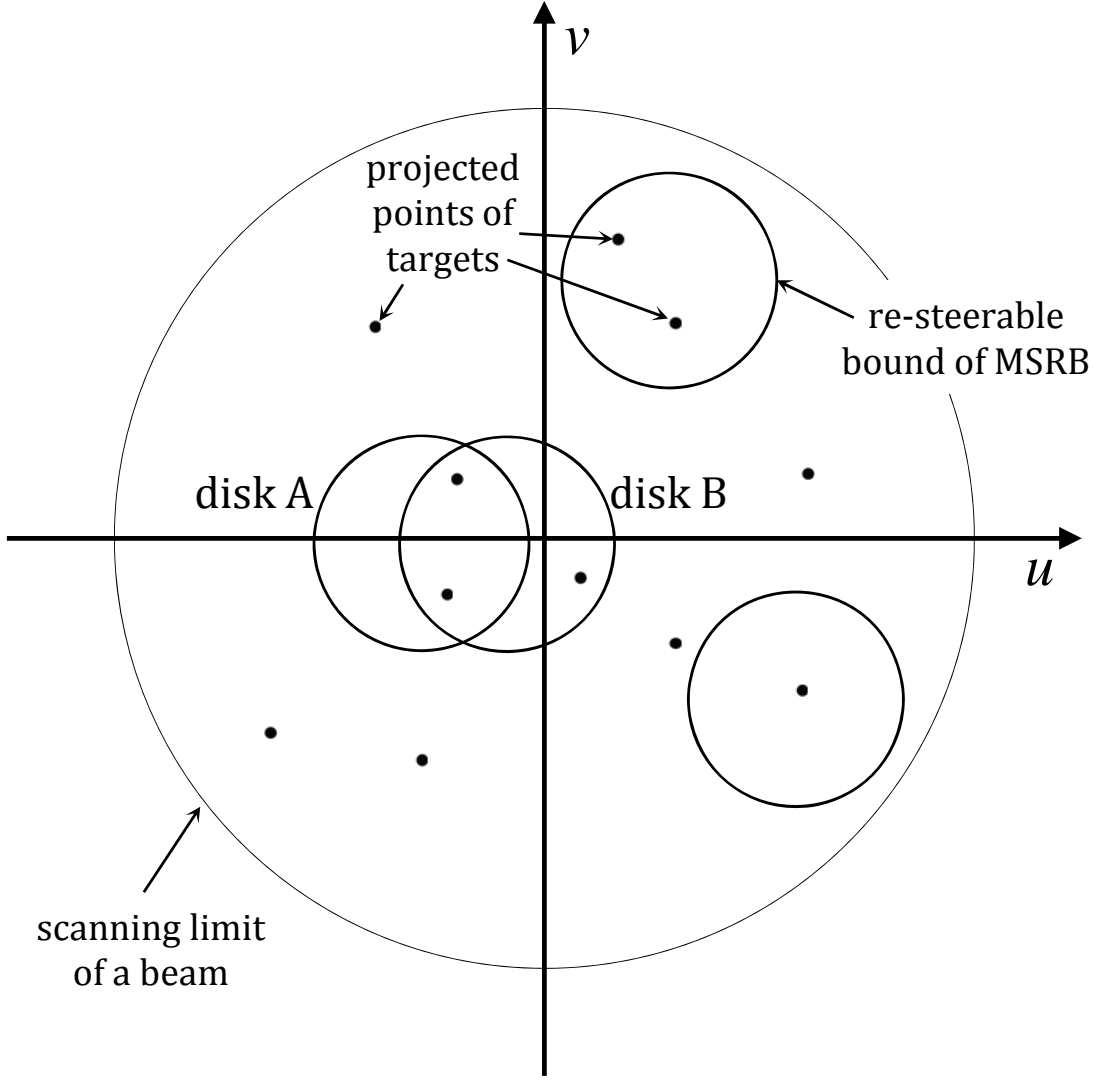


Fig. 3. Projected points of targets trackable with a PRF and circular re-steering boundaries of MSRB, i.e. the disks on the normalized scanning plane. u and v are the horizontal and vertical domains of the plane.

III. PROBLEM FORMULATION

Optimization problems to reduce tracking time in pulse interleaving with MSRB of both EDBF and SDBF are formulated in this section. The problem under EDBF is firstly considered as an integer program. The problem at SDBF is also represented by the same integer program, but groups of tasks that can be interleaved together have to be identified in advance.

For the both problems, each target is assumed to generate a single tracking task that consists of several looks with a PRF. If the periods of tracking tasks are similar and the requested intervals of execution of tasks are concentrated in a short time, at the time of tracking updates of all targets, pulses of some tasks are able to be interleaved with the same PRF. From this point, regardless of the number of looks contained in a single task, a interleaved group of looks is called simply an interleaved look or a look. In each PRI of a look, multiple consecutive positions of T-pulses can be specified since the T-pulses of

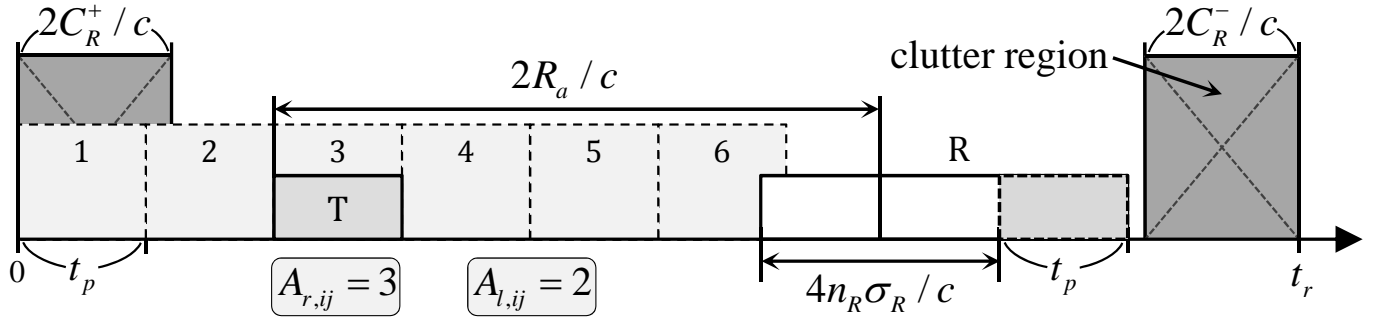


Fig. 4. The leftward availability $A_{l,ij}$ and the rightward availability $A_{r,ij}$ of the task i for the j th look. Two T-pulses of other tasks can be interleaved between T/R-pulses of the task i ($A_{l,ij}=2$), and the T-pulse of the task i can be shifted up to the third position ($A_{r,ij}=3$). The consecutive possible positions of T-pulses are expressed as light gray squares with dotted lines and marked with the position numbers.

different tasks are assumed to be successively positioned (see Fig. 4). If a T-pulse of a task is located in one of the positions in a PRI, all the same positions in all PRIs of the look is also occupied by the T-pulses of the same task since the pulses of the tasks are repeated with the same PRF in the interleaved look.

A. The Pulse Interleaving with EDBF

In the pulse interleaving problem with EDBF, for the i th target ($\equiv i$ th task) and the j th look with a PRF, $A_{v,ij}$ signifies availability of (i, j) pair. $A_{v,ij}$ is 1 if the target i satisfies (4) and (5) with the j th look's PRF, otherwise $A_{v,ij}$ is 0:

$$A_{v,ij} = \begin{cases} 1, & \text{if } (i, j) \text{ satisfies (4) and (5)} \\ 0, & \text{otherwise.} \end{cases} \quad (8)$$

A leftward availability $A_{l,ij}$ denotes the number of tasks whose T-pulses can be interleaved between T/R-pulses of the task i (see Fig. 4):

$$A_{l,ij} = A_{v,ij} \cdot \max \left(0, \left\lfloor \frac{2}{ct_p} (R_{a,ij} - n_R \sigma_{R,i} - \epsilon_R^+) \right\rfloor \right), \quad (9)$$

where $R_{a,ij}$ signifies the ambiguous range of the target i with the PRF of the j th look, and $\sigma_{R,i}$ is the standard deviation of the range of the target i . A rightward availability $A_{r,ij}$ denotes the number of positions counting rightward that the T-pulses of the task i can be shifted while keeping the task's R-pulses within the clear region (see Fig. 4):

$$A_{r,ij} = A_{v,ij} \cdot \max \left(0, \left\lfloor \frac{2}{ct_p} (R_u - (R_{a,ij} + n_R \sigma_{R,i} + \epsilon_R^-)) + 1 \right\rfloor \right). \quad (10)$$

Then, the pulse interleaving with MSRB of EDBF can be formulated as an integer program in **(IP)** through (C8). h_{ijk} and f_j are integer decision variables of the integer program **(IP)**. h_{ijk} is 1 when the

T-pulse of the i th tracking task is scheduled at the k th position of the j th look, and is 0 otherwise. f_j is 1 if there is at least one task assigned to the j th look. $t_{d,j}$ is the dwell time of the j th look. N_t and N_l are the number of tracking targets and the number of looks, respectively. N_{intlv} is the maximum number of tasks that can be interleaved in a single look and L_{inf} is an arbitrary large number. To obtain an optimal solution of pulse interleaving from the integer programming, a sufficient number of looks are specified for each PRF since multiple looks can be required to interleave multiple tasks trackable with a PRF: $N_{\text{PRF}} \leq N_l \leq N_{\text{PRF}} N_t$.

$$\underset{h_{ijk}, f_j}{\text{minimize}} \quad \sum_{j=1}^{N_l} t_{d,j} f_j \quad (\text{IP})$$

$$\text{subject to} \quad \sum_{i=1}^{N_t} \sum_{k=1}^{N_{\text{intlv}}} h_{ijk} \leq N_{\text{intlv}} f_j \quad (\text{C1})$$

$$\sum_{j=1}^{N_l} \sum_{k=1}^{N_{\text{intlv}}} h_{ijk} = 1 \quad (\text{C2})$$

$$\sum_{i=1}^{N_t} h_{ijk} \leq 1 \quad (\text{C3})$$

$$\sum_{i=1}^{N_t} (h_{ijk} - h_{ij(k+1)}) \geq 0 \quad (\text{C4})$$

$$\sum_{k=1}^{N_{\text{intlv}}} h_{ijk} \leq A_{v,ij} \quad (\text{C5})$$

$$\sum_{i=1}^{N_t} k \cdot h_{ijk} \leq \sum_{i=1}^{N_t} A_{r,ij} h_{ijk} \quad (\text{C6})$$

$$\sum_{i=1}^{N_t} \sum_{k=1}^{N_{\text{intlv}}} h_{ijk} \leq \sum_{i=1}^{N_t} (k + A_{l,ij}) h_{ijk} + L_{\text{inf}} (1 - \sum_{i=1}^{N_t} h_{ijk}) \quad (\text{C7})$$

$$h_{ijk} \in \{0, 1\}, \quad f_j \in \{0, 1\} \quad (\text{C8})$$

The objective of the integer program **(IP)** is to minimize the total tracking time, i.e. the sum of the dwell times for all the targets. The constraints of the problem are as follows: (C1) the number of tasks that can be interleaved in a single look is limited by N_{intlv} ; (C2) a task must be scheduled only one time; (C3) a position of a look can be designated to at most a single task; (C4) interleaved T-pulses in a PRI are placed successively; (C5) a task can be interleaved in a look with an available PRF of the task; (C6) the k th position of a look can be occupied by a T-pulse of a task whose $A_{r,ij}$ is larger than or equal to k ; (C7) all T-pulses of tasks interleaved in a look must not be overlapped with R-pulses of the tasks.

B. The Pulse Interleaving with SDBF

The looks in the integer program (**IP**) are characterized by only their PRFs in the pulse interleaving with EDBF. However, in the problem with SDBF, the geometric constraint in the normalized scanning plane introduced in II-B confines the looks to have disks in addition to PRFs: ‘*PRF selection*’ is transformed to ‘*disk selection*’. With the exception of the change in the characteristics of looks, the same form of the integer program as (**IP**) is utilized for the pulse interleaving problem with SDBF: $A_{v,ij}$ is 1 if the task i satisfies (4) and (5) with the j th look’s PRF and the projected target point of the task i is located in the disk of the j th look, otherwise $A_{v,ij}$ is 0; due to the change of $A_{v,ij}$, the values of $A_{l,ij}$ and $A_{r,ij}$ are also modified according to (9) and (10).

For solving the optimization problem efficiently, it is a prerequisite to search and obtain all possible looks without redundancy. If continuous beam pointing is available in the normalized scanning plane, there are an infinite number of disks that can be candidates to form the looks. Suppose a disk that encloses projected points of some targets on the normalized scanning plane is a set of the points. Then, all possible looks without redundancy are obtained from the minimal set of all unique equal-sized disks each of which is neither empty nor a proper subset of any disks. Therefore, any algorithm for searching the unique disks among infinite possibilities can reduce unnecessary computation.

This unique disk search is a preprocessing for solving pulse interleaving with SDBF by the integer program (**IP**) and it is closely related with the (geometric) unit disk cover problem [21], [22]. The definition of the discrete unit disk cover problem is as follows: given a set \mathcal{D} of unit disks and a set \mathcal{P} of points in the plane, find the minimum cardinality subset $\mathcal{D}' \subseteq \mathcal{D}$ such that every point in \mathcal{P} is enclosed by at least one disk in \mathcal{D}' . The continuous version has an infinite set of all unit disks confined in some areas of the plane. Thus, if the domain area of unit disks is a disk of radius larger than 1, the problem domain of the continuous unit disk cover is identical to the unique disk search. However, to the best of the author’s knowledge, any relation of unique disk search to the continuous unit disk cover has hardly received attention in the literature [21]–[26]. Since no algorithm to exactly obtain the unique disks is available in hand, the unique disks are approximately obtained by a brute force search from the disks on a rectangular grid (see section IV-B); as it is noted in section II-B, each PRF has a different set of projected points of trackable targets, and thus this procedure is repeated for each PRF.

Remark 1. Note that by excluding pulse scheduling in a look and by assuming any target has the maximum

left-/rightward availabilities if $A_{v,ij} = 1$, the integer program (**IP**) can be simplified as follows:

$$\text{minimize } \sum_j^{N_t} t_{d,j} f_j \quad (\mathbf{IP}_{\text{SSCFL}})$$

$$\text{subject to } \sum_i^{N_t} h_{ij} \leq N_{\text{intlv}} f_j \quad (11)$$

$$\sum_j^{N_t} h_{ij} = 1 \quad (12)$$

$$h_{ij} \leq A_{v,ij} \quad (13)$$

$$h_{ij} \in \{0, 1\}, f_j \in \{0, 1\} \quad (14)$$

This type of the problem is called the single-source capacitated facility location problem [27]. There are some previous works about exact solutions [28], [29] and heuristics [30], [31] for this NP-hard problem. A recent study [32] verifies local search algorithms using multi-exchange heuristic are effective for this problem.

IV. HEURISTIC ALGORITHMS

The integer program (**IP**) of the pulse interleaving with MSRB includes more complicated constraints than the single-source capacitated facility location problem, which is NP-hard. The integer programming for an optimal solution thus requires a high computational load with the increasing number of targets. However, since the ranges and frequencies of moving targets and corresponding available PRFs are vary with time, the pulse interleaving needs to be solved at every track update in multi-target tracking, where the update period is usually less than a few seconds. Not necessarily, a heuristic procedure for the pulse interleaving can be a practical solution in this case. In the following subsection, a heuristic pulse interleaving algorithm is presented for EDBF; a similar algorithm for SDBF is presented in IV-B; the time complexities of both algorithms are analyzed in V.

A. The Heuristic Algorithm for EDBF

The heuristic algorithm for EDBF consists of two phases: PRF selection of an interleaved look and scheduling of interleaved pulses in the look. The overall procedure of the algorithm is as follows. The algorithm repeatedly selects some PRF of a look, where pulse interleaving and scheduling are processed, until all tasks are assigned to looks. At every time a PRF is selected by a heuristic rule, pulses of some tasks are interleaved and scheduled along the positions in the look. The scheduling starts from the rightmost (latest) position and a task is selected by a heuristic rule for each position while the scheduling position

Algorithm 1 HeuristicInterleavingElementDBF

```

1: Load  $A_{v,in}$ ,  $A_{l,in}$ , and  $A_{r,in}$  for all  $(i, n)$  pairs.
2:  $H \leftarrow \phi$ 
3:  $T_0 \leftarrow$  the set of all tasks  $\equiv \{i | \forall i\}$ 
4:  $j \leftarrow 0$ 
5: while  $T_0 \neq \phi$  do
6:    $j \leftarrow j + 1$ 
7:    $p \leftarrow$  select a PRF by a heuristic rule (Heuristic of PRF selection).
8:    $T_p \leftarrow \{i | \forall i \in T_0, A_{v,ip} = 1\}$ 
9:    $S \leftarrow \phi$ 
10:   $S \leftarrow \text{BackwardInterleaving}(T_p, S, 1, N_{\text{intlv}}, p)$ 
11:   $T_0 \leftarrow T_0 \setminus \{i | \forall (i, k) \in S\}$ 
12:   $H \leftarrow H \cup \{(i, j, k) | \forall (i, k) \in S\}$ 
13: end while
14: return  $H$ 

```

translates backward (leftward). The two heuristic rules for the PRF and task selection in the algorithm are priority index based rules and thus the PRF/task with the maximum or minimum priority index are selected.

1) *Algorithm 1 - HeuristicInterleavingElementDBF*: Algorithm 1 and 2 are pseudocodes for the PRF selection and the pulse scheduling procedures, respectively. The presented heuristic algorithm starts from Algorithm 1 (**HeuristicInterleavingElementDBF** or **HIED**). First, the algorithm loads information of availabilities for all task-PRF (i, n) pairs: in the pseudocodes, $A_{v,in}$ denotes the availability of a task-PRF pair of task i and a look with PRF n , and $A_{l,in}$ and $A_{r,in}$ signify the leftward and rightward availabilities of the pair. The interleaving result H of the algorithm is composed of task indexes (i), look indexes (j), and interleaved positions (k). T_0 denotes the set of all tasks, which is contracted by removing scheduled tasks at the end of every while-loop of **HIED**. At every iteration of the while-loop, a PRF is selected by a PRF selection heuristic (Line 7). After PRF p of look j is selected, all tasks in T_0 trackable with p are assigned to T_p in Line 8 and then Algorithm 2 (**BackwardInterleaving** or **BI**) is called for the pulse scheduling in Line 10. As the result of the pulse scheduling in the look j , a schedule S is composed of tasks of interleaved pulses and corresponding positions. The scheduled tasks are eliminated from T_0 (Line 11) and triplets (i, j, k) of the scheduled tasks are inserted in H (Line 12). If T_0 becomes empty, then **HIED** returns H and terminates (Line 14).

2) *Algorithm 2 - BackwardInterleaving*: **BI** is called with the following input variables: the set of available (trackable) tasks T_a , a schedule S , the leftmost interleaving position E_l , the rightmost interleaving position E_r , and a selected PRF p . E_l and E_r are integer values denoting the position numbers. The present scheduling position and the rightmost scheduled (occupied) position are denoted by *cursor* and *tail*, respectively. *cursor* and *tail* are first set to E_r , i.e., the rightmost interleaving position of a corresponding

Algorithm 2 BackwardInterleaving(T_a, S, E_l, E_r, p)

```

1:  $tail \leftarrow E_r$ 
2: for  $cursor \leftarrow E_r$  to  $E_l$  step -1 do
3:    $T_l \leftarrow \{i | \forall i \in T_a, (tail - cursor) \leq A_{l,ip}\}$ 
4:    $A_{l,S} \leftarrow$  the leftward availability of schedule  $S$ 
5:   if  $T_l \neq \phi$  then
6:      $T_r \leftarrow \{i | \forall i \in T_l, cursor \leq A_{r,ip}\}$ 
7:     if  $T_r \neq \phi$  then
8:        $S \leftarrow$  schedule a task at  $cursor$  among the tasks in  $T_r$  by a heuristic rule (Heuristic of task selection).
9:        $T_a \leftarrow T_a \setminus \{i | \exists i, (i, cursor) \in S\}$ 
10:    else
11:      if  $cursor = E_r$  then
12:         $tail \leftarrow tail - 1$ 
13:      else
14:         $S \leftarrow$  shift all the pulses of tasks in  $S$  one step left.
15:         $S \leftarrow$  BackwardInterleaving( $T_a, S, tail, tail + \min(0, A_{l,S} - 1), p$ )
16:         $tail \leftarrow$  rightmost scheduled position in  $S$ 
17:      end if
18:    end if
19:  else
20:    if  $cursor \neq E_r$  then
21:       $S \leftarrow$  shift all the pulses of tasks in  $S$  to leftmost point.
22:       $S \leftarrow$  BackwardInterleaving( $T_a, S, E_l + tail - cursor, \min(tail, A_{l,S} + E_l + tail - cursor - 1), p$ )
23:      return  $S$ 
24:    end if
25:  end if
26: end for
27: return  $S$ 

```

call of **BI**. $cursor$ moves from E_r to E_l as the for-loop of **BI** is iterated (see Fig. 5a), and $tail$ is re-assigned right after the rightmost interleaving position is changed during the call (see Line 12 and 16 of **BI**).

In the for-loop of **BI**, two sets T_l , T_r and a value $A_{l,S}$ are calculated: T_l is the set of tasks whose leftward availabilities are larger than or equal to the present length of partial schedule, i.e. $(tail - cursor)$; T_r is the set of tasks that have rightward availabilities larger than or equal to the present $cursor$; $A_{l,S}$, the leftward availability of the present schedule S , denotes the number of positions where T-pulses of some tasks can be interleaved after the T-pulses of the tasks in S . There are three options according to the emptiness of T_l and T_r in the for-loop. If both T_l and T_r are not empty, there exists at least one task whose T-pulses can be interleaved at $cursor$, then a task is selected by a task selection heuristic (Line 8 and Fig. 5b). If T_l is not empty but T_r is empty, all the pulses of the tasks in S are shifted only one position left because there exist some tasks whose T-pulses can be interleaved with the pulses of the tasks in S at smaller $cursor$ (Line 14 and Fig. 5c). If T_l is empty, which means there is no task whose T-pulses and R-pulses

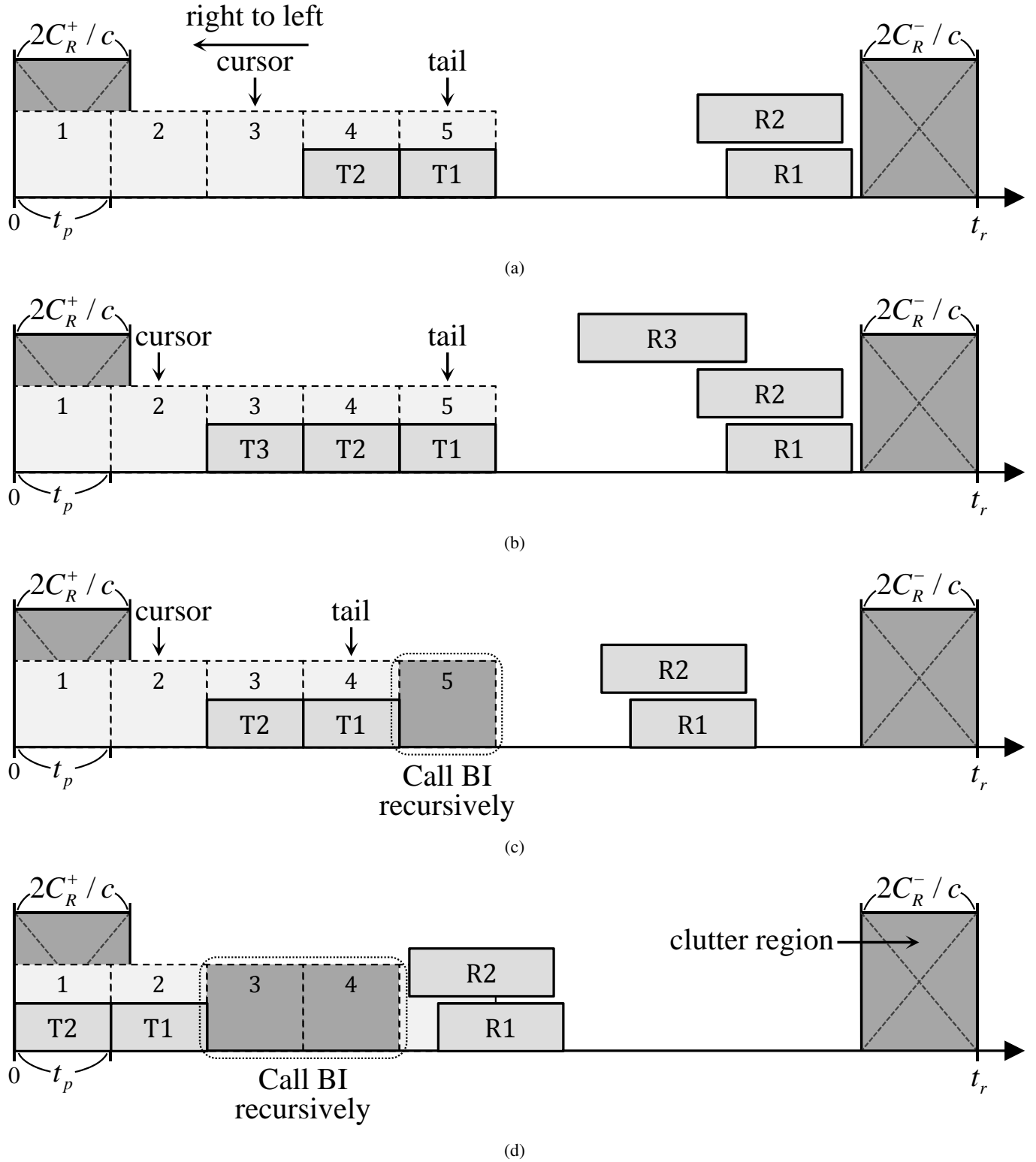


Fig. 5. A graphical interpretation of **BackwardInterleaving** algorithm: (a) *cursor*'s movement during iterations of the for-loop; (b) if $T_l \neq \phi$ and $T_r \neq \phi$, a task is selected by a task selection heuristic; (c) if $T_l \neq \phi$ and $T_r = \phi$, the pulses of tasks in S are shifted one position left; (d) if $T_l = \phi$, the pulses of tasks in S are shifted up to the leftmost position. T-/R-pulses of tasks are marked with 'T' and 'R' followed by the task numbers, and the consecutive possible positions of T-pulses are marked with the position numbers.

can be interleaved with T-pulses of the scheduled tasks, then all the pulses of the tasks in S are shifted up to the leftmost position (Line 21 and Fig. 5d). After the execution of each statement of the left shift,

another **BI** is called recursively with re-defined E_l and E_r (Line 15 and 22, and Fig. 5c and 5d). Since there are no T-pulses that need to be shifted when $cursor = E_r$, and thus the left shifts and the following recursive **BI**s are meaningless, the two statements of the left shifts are executed only if $cursor$ is not at E_r .

Since the scheduling in a look is processed backward (leftwards), the empty positions needed to consider on the right side of S are caused by only the left shifts. If the one-step left shift in Line 14 is executed several times during some iterations of the for-loop, multiple empty positions on the right side of S can be created. However, except the position next to S , the empty positions are no more considered, since it is already confirmed by the left shifts that no task exists satisfying the availabilities at those positions. Thus, after the one-step left shift of the schedule S , the algorithm allows at most a single task to be scheduled at the next right side position of S by setting $E_l = tail$ and $E_r = tail + \min(0, A_{l,S} - 1)$ at the recursive call of **BI** in Line 15.

On the other hand, If the algorithm shifts S up to the leftmost position, multiple positions can be cleared at one time. In this case, the positions after $tail$ are not needed to consider since the positions are confirmed to be unavailable by recursive calls of **BI** after the one-step left shifts. The right most position, where a T-pulse of a new task can be interleaved before R-pulses of tasks in S , is expressed by $A_{l,S} + E_l + tail - cursor - 1$ (see Fig. 5d). Therefore, **BI** is called recursively with the empty positions from the next right side position of S , i.e. $E_l + tail - cursor$ to the position of the minimum value between $tail$ and $A_{l,S} + E_l + tail - cursor - 1$ in Line 22.

3) PRF and Task Selection Heuristics: A PRF of an interleaved look in the while-loop of **HIED** and a task scheduled in the for-loop of **BI** are selected by priority index based heuristic rules. In this paper, greedy (G), reverse greedy (RG) and random (R_{PRF}) selections are used for the PRF selection heuristics in Line 7 of **HIED**. The greedy heuristic is a well-known $\log n$ -approximation algorithm for the set-cover problem and it is also proved as a $\log n$ -approximation algorithm for the general uncapacitated facility location problem [33]. In every iteration of the while-loop in **HIED**, the greedy heuristic selects a PRF with the maximum number of unscheduled targets that can be tracked with the PRF. The reverse greedy and the random rules are used for comparison: the reverse greedy selects a PRF with the minimum number of trackable targets, and the random rules selects a PRF randomly.

For the task selection heuristics in Line 8 of **BI**, 6 priority index based rules are used:

- shortest ambiguous range first (SAR): select a task of a target with the smallest R_a .
- longest ambiguous range first (LAR): select a task of a target with the largest R_a .
- random (R_{task}): select a task randomly.
- smallest number of available PRFs first (SAP): select a task with the smallest number of PRFs that

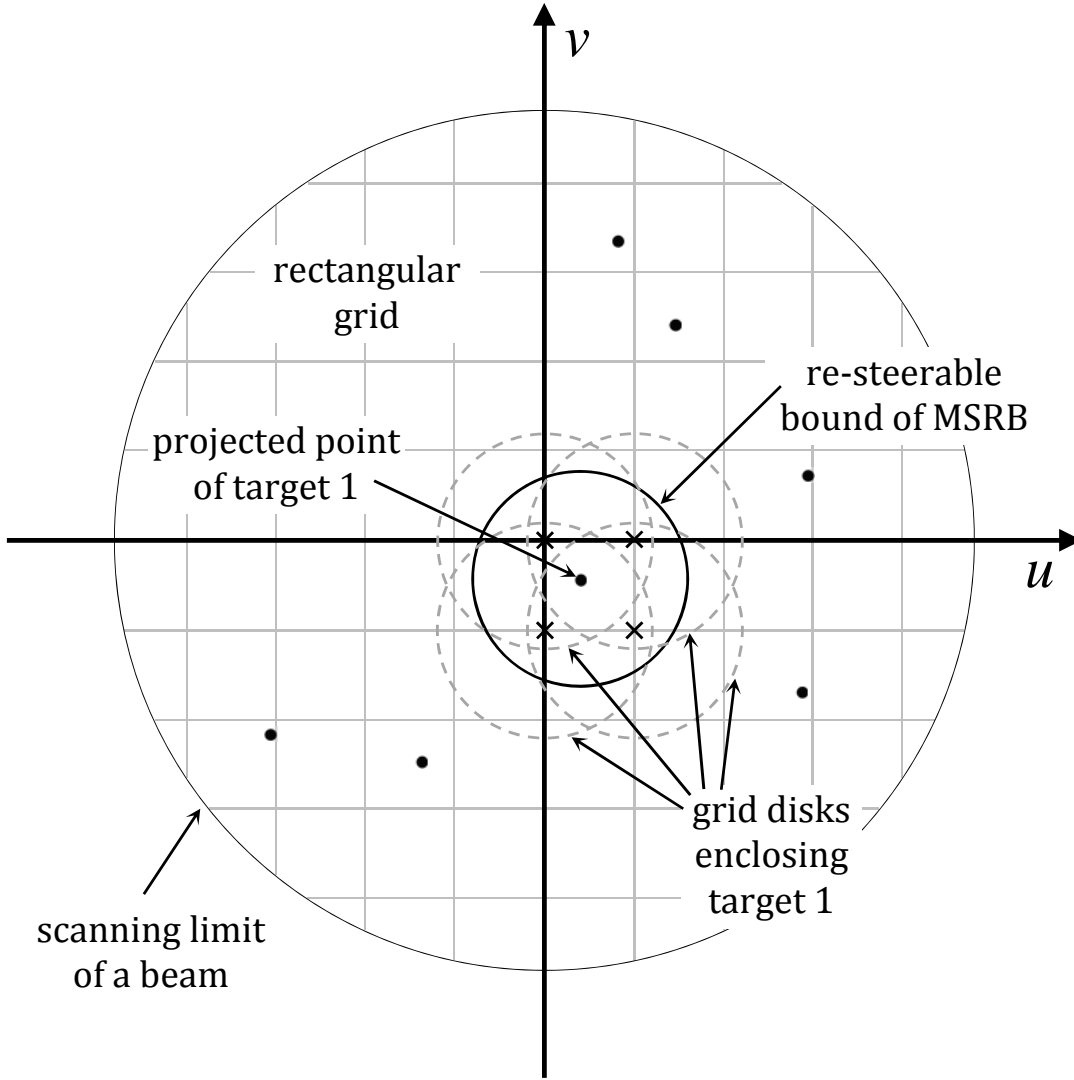


Fig. 6. The grid disks (dotted gray) enclosing a projected point of a target trackable with a PRF: the grid points of a rectangular grid within the disk (\equiv the re-steerable bound of MSRB) radius from the projected target point are utilized as the grid disk centers (marked as X). u and v are the horizontal and vertical domains of the plane.

the task can be performed with.

- smallest leftward availability first (SLA): select a task with the smallest sum of its leftward availabilities for all PRFs.
- smallest rightward availability first (SRA): select a task with the smallest sum of its rightward availabilities for all PRFs.

B. The Heuristic Algorithm for SDBF

The heuristic interleaving algorithm for SDBF is characterized by preprocessing of grid disks and disk selection of an interleaved look, compared with the algorithm for EDBF. A disk is a re-steerable area of MSRB centered on a point in the normalized scanning plane. The center of a disk can be located at an almost infinite number of points depending on the beam pointing capability of a radar. For celerity rather

Algorithm 3 HeuristicInterleavingSubarrayDBF

```

1: Load  $A_{v,in}$ ,  $A_{l,in}$ , and  $A_{r,in}$  for all  $(i, n)$  pairs.
2: for  $p \leftarrow 1$  to  $N_{PRF}$  do
3:    $T_{v,p} \leftarrow \{i | \forall i, A_{v,ip} = 1\}$ 
4:   for  $i \in T_{v,p}$  do
5:      $D_i \leftarrow \{d | \forall d, p_d = p, \|g_d - q_i\| \leq r\}$ 
6:     for  $d \in D_i$  do
7:       Add  $i$  to  $T_d$ , the set of tasks enclosed by  $d$ .
8:     end for
9:   end for
10: end for
11:  $H \leftarrow \phi$ 
12:  $T_0 \leftarrow$  the set of all tasks  $\equiv \{i | \forall i\}$ 
13:  $j \leftarrow 0$ 
14: while  $T_0 \neq \phi$  do
15:    $j \leftarrow j + 1$ 
16:    $d \leftarrow$  select a disk by a heuristic rule (Heuristic of disk selection).
17:    $S \leftarrow \phi$ 
18:    $S \leftarrow \text{BackwardInterleaving}(T_d, S, 1, N_{intlv}, p_d)$ 
19:    $T_0 \leftarrow T_0 \setminus \{i | \forall (i, k) \in S\}$ 
20:    $T_d \leftarrow T_d \setminus \{i | \forall (i, k) \in S\}$ 
21:    $H \leftarrow H \cup \{(i, j, k) | \forall (i, k) \in S\}$ 
22: end while
23: return  $H$ 

```

than exactitude, an imaginary rectangular grid on the normalized scanning plane is adopted to generate a finite number of disk centers as an approximated set of the original infinite centers. The grid points within the disk radius from any projected target point on the normalized scanning plane are utilized as disk centers for the heuristic pulse interleaving (see Fig. 6). After the preprocessing of grid disks for each PRF, the algorithm repeatedly selects some disks according to a heuristic rule until all tasks are assigned. The pulse scheduling procedure in a look with a selected disk is the same as the EDBF case.

1) *Algorithm 3 - HeuristicInterleavingSubarrayDBF*: Algorithm 3 (**HeuristicInterleavingSubarrayDBF** or **HISD**) is a pseudocode for the preprocessing of grid disks and the disk selection. After information of the availabilities for all task-PRF (i, n) pairs is loaded in Line 1 of **HISD**, grid disks that enclose at least one projected target point are identified in the following cascade of for-loops (Line 2-10). If the projected target point q_i of task i is within the disk radius r from the center g_d of grid disk d and the task i is trackable with the PRF p_d of the disk d , the projected target point q_i of the task i is enclosed by the disk d centered on g_d in the normalized scanning plane. D_i denotes the set of grid disks that enclose the projected target point of the task i . To identify all nonempty grid disks for each PRF, **HISD** inserts projected target points of tasks in the normalized scanning plane one by one, determines D_i (Line 5), and adds the task index to a task list T_d for each disk in D_i (Line 7).

The grid disks identified in **HISD** are inherently duplicative: since a single projected target point can be enclosed by multiple grid disks, multiple disks can have the same task list T_d . The disks are arranged to distinguish the unique disks for the integer program. However, duplicative disks are allowed for the heuristic algorithms since a priority index based disk selection heuristic selects a disk among the ‘best’ disks and scheduled tasks are eliminated from the task lists of all the disks after the pulse scheduling (Line 20). The retention of the duplicative disks increases the computational load in the while-loop of **HISD**, but a larger computation is required to discriminate supersets among the disks for unique disk search.

After the grid disks are created, the interleaving result H , the set of all tasks T_0 , and look index j are initialized in Line 11-13. At every iteration of the while-loop in **HISD**, a disk, whose PRF and look index are p_d and j , is selected by a disk selection heuristic in Line 16, and then **BI** is called for the pulse scheduling in Line 18, as is the case in EDBF. The scheduled tasks in S are eliminated from T_0 and T_d after the pulse scheduling, and triplets (i, j, k) of the scheduled tasks are inserted in H (Line 19-21). Repeating this procedure in the while-loop, if T_0 becomes empty, then **HISD** returns H and terminates.

2) *Disk Selection Heuristics*: The disk selection heuristic in **HISD** consists of two priority indexes: a main index and a sub-index for tie-breaking. As main indexes, greedy disk (GD), reverse greedy disk (RGD), and weighted greedy disk (WGD) selections are used in this paper. GD selects a disk of the maximum cardinality, i.e. the maximum number of enclosed tasks, whereas RGD selects a disk of the minimum cardinality. In WGD, a disk of the maximum weighted cardinality is selected, where the weight is the sum of the reciprocal of the number of available disks of each target enclosed by the disk. Since there can exist many disks of the same cardinality, including duplicates, at least randomized tie-breaking is needed to avoid initial biases. The sub-indexes used for tie-breaking are random (R_{disk}) and smallest dwell time first (SD). R_{disk} is random selection of disks among the disks with the same value of the main index, and SD selects a disk whose look has smallest dwell time among the disks: the latter is for reducing the total tracking time as far as possible.

V. ALGORITHM COMPLEXITY ANALYSIS

The asymptotic time complexities of the interleaving algorithms are analyzed in this section. The algorithms can be implemented in several ways with some data structures for the PRF/disk and task selection heuristics. The PRF selection heuristics use the cardinality of the set of unscheduled tasks trackable with a PRF p , i.e. $|T_p|$ as the priority index for G and RG, or generate random numbers for R_{PRF} . Since the priority index for G and RG is an integer and increases/decreases with insertion/deletion of tasks, it will be shown in the following subsection that G and RG, as in random number generation, take $O(1)$ time with a particular sorted list. By the same token, disk selection heuristics based on GD or

RGD as the main index and R_{disk} as the sub-index require constant time for each execution (see V-D). But, if the disk heuristic uses a continuous priority index (WGD) or a sub-index that requires comparison operations (SD), a search tree is needed for an efficient computation (see V-D). In **BI**, a task among the tasks in T_r is selected so that pulses of the task are interleaved, and thus a task selection heuristic based on priority index must be valid in different sets of tasks, i.e. T_l s and T_r s. Three options for the task selection are analyzed in this paper : brute force search through an unsorted task list (V-A), selection from $N_{\text{intlv}}(N_{\text{intlv}} - 1)$ sorted task lists of all pairs of (T_l, T_r) for each PRF (V-B), and multi-level search by 3-dimensional orthogonal range trees (V-C).

A. The Algorithm for EDBF with Brute Force Search

First, the time complexity of the pulse interleaving algorithm for EDBF using the brute force search is analyzed. In **HIED**, to load and calculate availabilities of all task-PRF pairs, $O(N_t N_{\text{PRF}})$ time is spent (Line 1). The initiation of T_0 in Line 3 requires $O(N_t)$ time computation, and the while-loop runs at most N_t times in the worst cases. For PRF selection heuristics, a sorted list of PRFs whose length is N_{PRF} is used. Each of the PRFs in the list has a pointer to a value of $|T_p|$ and vice versa, and thus multiple PRFs of equal $|T_p|$ s can have the same pointers. Each value of $|T_p|$ appended to the list is mutually connected with the next larger value and the next smaller value; the maximum and the minimum value of $|T_p|$ have self-pointing addresses. Initially, all PRFs point to 0, and inserting tasks one by one, the pointer of every PRF available for the inserted task moves to the value of $|T_p|$ increased by 1. If the value does not exist, then it is created and connected to the PRF's former value of $|T_p|$ and the next larger value. When a value of $|T_p|$ has no pointer to any PRFs, the value is deleted and the next larger and smaller values of it are mutually connected. The computation time for this preprocessing is proportional to $\sum_{p=1}^{N_{\text{PRF}}} |K_p|$, hereafter denoted by Q_p , where K_p is the set of all tasks trackable with a PRF p . The PRF heuristic selects one of the PRFs with the largest value of the list (G) or with the smallest value (RG) and thus it takes $O(1)$ time. During the preprocessing, the task list T_p of each PRF is also constructed within the same complexity Q_p and every task is mutually connected with its available PRFs for task deletion. By the task deletion from T_p after every pulse scheduling in a look, no extra operation is needed for Line 8.

Proposition 1. The sorted list of PRFs with the cardinalities of their trackable tasks for constant time PRF selection can be constructed in $O(\sum_{p=1}^{N_{\text{PRF}}} |K_p|) = O(Q_p)$ time, and a corresponding task list can be constructed in $O(Q_p)$ time.

At every call of **BI** from Line 10 in **HIED**, the for-loop of **BI** runs exactly N_{intlv} times unless the forced return in Line 23 of **BI** is executed. Since a recursive call of **BI** in Line 15 is with at most a single interleaving position, the recursive **BI** ends in a single for-loop and the corresponding position is

occupied or abandoned in the further process. Therefore, this recursion additionally iterates the for-loop at most N_{intlv} times during a call of **BI** from **HIED**. On the other hand, the recursive call of **BI** in Line 22 does not increase the total iteration of the for-loop since the call of **BI** in Line 22 is with unvisited remaining interleaving positions after the total left shift and the algorithm returns right after Line 22.

Proposition 2. The for-loop of **BI** iterates at most $2N_{\text{intlv}}$ times during a call of **BI** from **HIED**.

As a task i is selected in Line 8 of **BI**, the new value of $A_{l,S}$ is the minimum between the previous $A_{l,S}$ and $A_{l,ip} - (\text{tail} - \text{cursor})$: the latter is the number of positions between the T-pulses of the present schedule S and the R-pulse of i . Therefore, $A_{l,S}$ in Line 4, which is initially N_{intlv} by definition, can be updated in $O(1)$ time after every task selection. The left shifts in Line 14 and 21 can be done in $O(1)$ by an appropriate list of pointers for interleaved positions and corresponding tasks in S : since S is composed of at most two lists of tasks whose T-pulses are consecutive by the left shifts, 4 pointers for both ends of the two task lists are enough to represent and manipulate interleaved positions for the shifts.

T_l and T_r are the sets of tasks used for emptiness check in if-statements of **BI** and heuristic task selection. Thus, a list of tasks that satisfy the conditions of T_l and T_r is required to be identified for the task selection. In brute force search, in every iteration of the for-loop of **BI**, all the tasks in T_a are checked whether they satisfy the conditions of T_l and T_r in order, and then a task with the maximum priority index among the tasks in T_r is searched and selected. Therefore, the operations for brute force search require $O(|T_p|)$ time in the worst cases.

Proposition 3. A call of **BI** from **HIED** totally requires $O(N_{\text{intlv}}|T_p|_{\max})$ time by the brute force search even in the worst cases, where $|T_p|_{\max} \equiv \max_p |T_p|$.

Proof: Since it is already shown that other operations in the for-loop of **BI** except the brute force search takes $O(1)$ time, the time complexity of a single execution of the for-loop is $O(|T_p|)$ in summary. By Proposition 2, the number of iterations of the for-loop is $O(N_{\text{intlv}})$, and thus a call of **BI** from **HIED** takes $O(N_{\text{intlv}}|T_p|_{\max})$ time by the brute force search even in the worst cases ■

After the pulse scheduling in a look, the scheduled tasks are deleted from T_p s of all PRFs and T_0 , and merged into H : the time for merge of each task is trivially $O(1)$. Since a task is mutually connected to all available PRFs, the deletion takes $O(|P_i| + 1)$ time, where P_i denotes the set of available PRFs of task i . The deletion of the task reduces $|T_p|$ of the corresponding PRFs, and therefore the pointers of the PRFs are moved to the values decreased by 1 in the sorted PRF list; all the related operations are similar to the preprocessing.

Lemma 1. The time complexity of the pulse interleaving algorithm for EDBF using the brute force search is $O(N_t(N_{\text{PRF}} + N_{\text{intlv}}|K_p|_{\max}))$, where $|K_p|_{\max} \equiv \max_p |K_p|$.

Proof: The sum of the cardinalities of all K_p s and the sum of the cardinalities of all P_i s are the same: $\sum_{p=1}^{N_{\text{PRF}}} |K_p| = \sum_{i=1}^{N_t} |P_i| = Q_p$. The deletion and the merge occur, respectively, only one time per task, and thus Q_p computation time is needed during the entire algorithm execution. The calculations for the availabilities of all task-PRF pairs takes $O(N_t N_{\text{PRF}})$ time, and the while-loop of **HIED** runs at most N_t times. Therefore, by Proposition 1 and 3, the time complexity of the algorithm with the brute force search is $O(N_t N_{\text{PRF}} + N_t \cdot N_{\text{intlv}} |K_p|_{\max} + Q_p) = O(N_t (N_{\text{PRF}} + N_{\text{intlv}} |K_p|_{\max}))$ since $T_p \subseteq K_p$ and $Q_p \leq N_t N_{\text{PRF}}$. ■

B. Sorted Task Lists

The second option of the data structure for the task selection heuristics is to prepare a sorted task list for each pair of (T_l, T_r) . By the definition in Line 3 and Line 6 of **BI**, T_l and T_r are the sets of tasks whose $A_{l,ip}$ and $A_{r,ip}$ are larger than certain positive integers, respectively. Since $0 \leq A_{l,ip} \leq N_{\text{intlv}}$ and $1 \leq A_{r,ip} \leq N_{\text{intlv}}$ for a task $i \in K_p$, there are $N_{\text{intlv}}(N_{\text{intlv}} - 1)$ possible pairs of (T_l, T_r) . In the preprocessing of the second option, the tasks satisfying the conditions of each (T_l, T_r) pair are sorted according to a priority index of a task selection heuristic: it is done in $O(|K_p| \log |K_p|)$ time. For all PRFs and all (T_l, T_r) pairs, the time complexity of the preprocessing is $O(\sum_{p=1}^{N_{\text{PRF}}} (|K_p| \log |K_p|) N_{\text{intlv}}^2)$ or less tightly $O(Q_p \log |K_p|_{\max} N_{\text{intlv}}^2)$.

The complexities of most operations in the algorithm are the same as the brute force search except the identification of T_l and T_r (Line 3 and 6 of **BI**) and task selection and deletion (Line 8 and 9 of **BI** and Line 11 of **HIED**).

Proposition 4. The time complexity of a call of **BI** from **HIED** is $O(N_{\text{intlv}}^2 N_s)$, where N_s denotes the number of scheduled tasks in the call.

Proof: Since T_l and T_r are identified in advance, no extra operation is needed for Line 3, and 6 of **BI** and task selection is also done in $O(1)$ time from the sorted list. However, a selected task has to be deleted from all $N_{\text{intlv}}(N_{\text{intlv}} - 1)$ sorted lists of the selected look's PRF. The deletion can be processed in $O(N_{\text{intlv}}^2)$ time with the task's pointers to the task lists, and thus the deletion of all scheduled tasks takes $O(N_{\text{intlv}}^2 N_s)$ during a call of **BI** from **HIED**. Since other operations in **BI** takes $O(1)$ time for each iteration of the for-loop, and by Proposition 2, the time complexity of a call of **BI** from **HIED** is $O(N_{\text{intlv}}^2 N_s)$. ■

Lemma 2. The time complexity of the pulse interleaving algorithm for EDBF using multiple sorted task lists is $O(N_t N_{\text{PRF}} + Q_p \log |K_p|_{\max} N_{\text{intlv}}^2)$.

Proof: For each scheduled task, the deletion from the task lists of other PRFs is also required after pulse scheduling: the time complexity is $O(|P_i| N_{\text{intlv}}^2)$ per task. Therefore, the task deletion through the

algorithm requires $O(\sum_{i=1}^{N_t} |P_i| N_{\text{intlv}}^2) = O(Q_p N_{\text{intlv}}^2)$ time. Since a task is scheduled only one time in the algorithm, the time spent by all the calls of **BI** from **HIED** is $O(N_t N_{\text{intlv}}^2)$. The calculations for the availabilities of all task-PRF pairs takes $O(N_t N_{\text{PRF}})$ time, and the time complexity of the preprocessing for the sorted task lists is $O(Q_p \log |K_p|_{\max} N_{\text{intlv}}^2)$. In summary, the time complexity of the algorithm using multiple sorted task lists is $O(N_t N_{\text{PRF}} + Q_p \log |K_p|_{\max} N_{\text{intlv}}^2 + N_t N_{\text{intlv}}^2 + Q_p N_{\text{intlv}}^2) = O(N_t N_{\text{PRF}} + Q_p \log |K_p|_{\max} N_{\text{intlv}}^2)$ since $Q_p \geq N_t$. ■

C. A Multi-Level Search by Orthogonal Range Trees

The sorted task lists for task selection can be stored more efficiently by orthogonal range trees. Since a task with the maximum priority index is selected among the tasks whose $A_{l,ip}$ and $A_{r,ip}$ are larger than certain positive integers, a data structure is utilizable that can efficiently answer orthogonal rectangular range queries in the $A_{l,ip}-A_{r,ip}$ plane and efficiently report a task with the maximum priority index from the query result. A 3-dimensional orthogonal range tree is appropriate for the requirements: the first level of this range tree is a balanced binary search tree of $A_{l,ip}$; for each node in the first level tree, an auxiliary search tree of $A_{r,ip}$ is built as the second level tree; the last level of the range tree needs not to be a search tree but just to be a sorted list of tasks according to a priority index.

Proposition 5. The orthogonal range tree can answer the task selection/deletion query in $O(\log^2 N_{\text{intlv}})$ time and can be built in $O(|K_p|(\log |K_p| + \log^2 N_{\text{intlv}}))$ time for each PRF.

Proof: The depths of the first and second level trees are at most $\log N_{\text{intlv}}$ since $A_{l,ip}$ and $A_{r,ip}$ are positive integers no larger than N_{intlv} . Then, the preprocessing for the range trees is as follows. First, for each PRF, sort tasks by a priority index of a task selection heuristic in $O(|K_p| \log |K_p|)$ time. Then, insert the tasks to the range tree in the sorted order in $O(|K_p| \log^2 N_{\text{intlv}})$ time. As a result, the tasks at the third level in each node of the second level search tree are naturally sorted.

Using this orthogonal range tree, the identification of T_l and T_r in **BI** can be done in $O(\log N_{\text{intlv}})$ and $O(\log^2 N_{\text{intlv}})$, respectively. To acquire the best task according to the priority index, all the best tasks from task lists of $\log^2 N_{\text{intlv}}$ nodes of the second level trees, reported by the range query of T_r , are compared. Obviously, this comparison is done in $O(\log^2 N_{\text{intlv}})$ time. The deletion of the selected task is processed in $O(\log^2 N_{\text{intlv}})$ time since the task is contained in $\log^2 N_{\text{intlv}}$ nodes through the orthogonal range tree. Therefore, the task selection followed by the deletion is processed in $O(\log^2 N_{\text{intlv}})$ time. ■

Proposition 6. The time complexity of a call of **BI** from **HIED** is $O(N_{\text{intlv}} \log^2 N_{\text{intlv}})$.

Proof: The identification of T_r can occur in every iteration of the for-loop of **BI**, which takes $O(N_{\text{intlv}} \log^2 N_{\text{intlv}})$ in total, whereas the task selection and deletion are processed $N_s (\leq N_{\text{intlv}})$ times.

Other operations in **BI** takes $O(1)$ time for each iteration of the for-loop, and thus the proposition is concluded. ■

Lemma 3. The time complexity of the pulse interleaving algorithm for EDBF using orthogonal range trees is $O(N_t N_{\text{PRF}} + Q_p(\log |K_p|_{\max} + \log^2 N_{\text{intlv}}) + N_t N_{\text{intlv}} \log^2 N_{\text{intlv}})$.

Proof: The scheduled tasks are deleted from the orthogonal range trees of other PRFs after the pulse scheduling and the time complexity of this deletion is $O(|P_i| \log^2 N_{\text{intlv}})$ per task. This task deletion through the algorithm takes $O(\sum_{i=1}^{N_t} |P_i| \log^2 N_{\text{intlv}}) = O(Q_p \log^2 N_{\text{intlv}})$ time. Since the while-loop of **HIED** runs at most N_t times, the time spent by all the calls of **BI** from **HIED** is $O(N_t N_{\text{intlv}} \log^2 N_{\text{intlv}})$ by Proposition 6. The calculations for the availabilities of all task-PRF pairs takes $O(N_t N_{\text{PRF}})$ time, and the time complexity of the preprocessing for the orthogonal range trees for all PRFs is $O(Q_p(\log |K_p|_{\max} + \log^2 N_{\text{intlv}}))$ by Proposition 5. In summary, the time complexity of the algorithm using orthogonal range trees is $O(N_t N_{\text{PRF}} + Q_p(\log |K_p|_{\max} + \log^2 N_{\text{intlv}}) + N_t N_{\text{intlv}} \log^2 N_{\text{intlv}})$. ■

With a small constant N_{intlv} , as a reasonable assumption with a high duty ratio (see II-B), $N_t N_{\text{intlv}} \leq Q_p \log |K_p|_{\max}$. Thus, Lemma 3 shows that, In comparison with the algorithm using multiple sorted lists, the algorithm runs faster by orthogonal range trees in terms of the asymptotic complexity.

The time complexities shown in Lemma 2 and 3 can be simplified with some constant parameters and a scalable number of targets.

Theorem 1. The time complexity of the pulse interleaving algorithm for EDBF using multiple sorted task lists or orthogonal range trees is $O(N_t \log N_t)$ if N_{PRF} and N_{intlv} are constant.

Proof: Since $|K_p|_{\max} \leq N_t$, if N_{PRF} and N_{intlv} are constant, then $O(Q_p) \leq O(N_t N_{\text{PRF}}) = O(N_t)$ and the complexities in Lemma 2 and 3 are reduced to $O(N_t \log N_t)$. ■

D. The Algorithm for SDBF

The main difference between two heuristic interleaving algorithms for EDBF and SDBF is the change in the characteristics of looks. A look has a PRF without any geometric constraints in the former, whereas a look is confined to have a disk in addition to a PRF in the latter. Furthermore, the heuristic interleaving algorithm for SDBF produces a number of grid disks, which increase the computation time and require extra data structures. The grid disks are created in the preprocessing by inserting the projected target points of the tasks on the normalized scanning plane for each PRF. The grid points of a rectangular grid with a spacing ϵ can be the centers of the grid disks created by an inserted task's projected target point if the point is located within the disk radius r from the grid points (see Fig. 6).

Thus, the preprocessing of grid disks is as follows. First, for each PRF, inserting trackable tasks one by one, the region of grid disk centers enclosed by a disk, whose radius is r and whose center is the

projected target point q_i of the inserted task i , is calculated. The region consists of $\lfloor \frac{2r}{\epsilon} \rfloor$ row intervals of abscissa or column intervals of ordinate. Then, two data structures are built for the grid disks during the insertion of tasks. The first is a search tree of the grid disks, for each PRF, sorted lexicographically by the coordinates of the disks' centers. This search tree is to identify whether the disks already exist whose centers are in the region of grid disk centers from a new task insertion. The second is a sorted list of the disks for all PRFs according to the cardinality of disk: the list has the same structure as the one used for PRF selection heuristics.

Let $N_{d,p}$ denote the number of grid disks for PRF p , $N_d (\equiv \sum_{p=1}^{N_{\text{PRF}}} N_{d,p})$ be the number of grid disks of all PRFs, K_d be the set of all tasks trackable in a disk d , and Q_d denote the sum of the cardinalities of all K_d s, i.e. $\sum_{d=1}^{N_d} |K_d|$.

Proposition 7. The search trees and the sorted list for grid disks are constructed in $O(N_d \log N_{d,p}|_{\max} + Q_d)$ time.

Proof: The search trees are constructed during the preprocessing of the grid disks to identify existing grid disks in the trees by previous task insertions. Since the region of grid disk centers are calculated in a constant time for each task insertion and each identified grid disk d encloses $|K_d|$ projected target points, at least $O(Q_d)$ time is required for identifying the grid disks in the preprocessing. The search tree of each PRF is obviously constructed in $O(N_{d,p} \log N_{d,p})$ time, and thus the processing of all of those trees requires $O(\sum_{p=1}^{N_{\text{PRF}}} (N_{d,p} \log N_{d,p}))$ time or less tightly $O(N_d \log N_{d,p}|_{\max})$ for all PRFs. By the same way of constructing the sorted list of PRFs in V-A, the sorted list of the grid disks for all PRFs with their cardinality is constructed in $O(Q_d)$ time. Thus, the two types of the structures are constructed in $O(N_d \log N_{d,p}|_{\max} + Q_d)$. ■

For WGD, the weight of a disk, i.e. the sum of the reciprocal of the number of available disks for the tasks enclosed by the disk is also calculated. Since the number of available disks of a task is trivially known through the task insertion, no extra complexity increases. However, the disks are must be sorted by the continuous weighted cardinality in $O(N_d \log N_d)$ time. Any sub-index of a disk selection heuristic except random selection also needs sorting of disks, and thus $O(N_d \log N_d)$ computation is required.

The number $N_{d,p}$ of grid disks for PRF p is proportional to the disk area, the density of grid points, and the number of the task insertions, and thus $N_{d,p} = O(\frac{r^2}{\epsilon^2} |K_p|)$. Therefore, the following proposition is derived.

Proposition 8. The time complexity of the preprocessing for the grid disks is $O(\frac{r^2}{\epsilon^2} Q_p \log \frac{r^2}{\epsilon^2} |K_p|_{\max} + Q_d)$ if GD or RGD without any sub-index is used for a disk selection heuristic, and it is $O(\frac{r^2}{\epsilon^2} Q_p \log \frac{r^2}{\epsilon^2} Q_p + Q_d)$ if WGD or any sub-index is used for a disk selection heuristic.

Proof: If GD or RGD without any sub-index is used for a disk selection heuristic, by Proposition 7, the time complexity of the preprocessing for grid disks is $O(\frac{r^2}{\epsilon^2}Q_p \log \frac{r^2}{\epsilon^2}|K_p|_{\max} + Q_d)$, since $N_d = \sum_{p=1}^{N_{\text{PRF}}} N_{d,p} = O(\sum_{p=1}^{N_{\text{PRF}}} \frac{r^2}{\epsilon^2}|K_p|) = O(\frac{r^2}{\epsilon^2}Q_p)$. By the same token, if WGD or any sub-index is used for a disk selection heuristic, the complexity $O(N_d \log N_d + Q_d)$ becomes $O(\frac{r^2}{\epsilon^2}Q_p \log \frac{r^2}{\epsilon^2}Q_p + Q_d)$. ■

For other operations, the same complexity analysis can be applied, except some notions are changed from K_p and Q_p to T_d and Q_d . Therefore, the time complexities of the pulse interleaving algorithm for SDBF using different data structures are arranged as the following lemma.

Lemma 4. The time complexities of the pulse interleaving algorithm for SDBF are summarized as follows:

- 1) brute force search: $O(N_t(N_{\text{PRF}} + N_{\text{intlv}}|K_d|_{\max}) + Q_d + \frac{r^2}{\epsilon^2}Q_p \log \frac{r^2}{\epsilon^2}|K_p|_{\max})$
- 2) sorted task lists: $O(N_t N_{\text{PRF}} + Q_d \log |K_d|_{\max} N_{\text{intlv}}^2 + \frac{r^2}{\epsilon^2}Q_p \log \frac{r^2}{\epsilon^2}|K_p|_{\max})$
- 3) orthogonal range trees: $O(N_t N_{\text{PRF}} + Q_d(\log |K_d|_{\max} + \log^2 N_{\text{intlv}}) + N_t N_{\text{intlv}} \log^2 N_{\text{intlv}} + \frac{r^2}{\epsilon^2}Q_p \log \frac{r^2}{\epsilon^2}|K_p|_{\max})$.

The last term $\frac{r^2}{\epsilon^2}Q_p \log \frac{r^2}{\epsilon^2}|K_p|_{\max}$ of each expression is changed to $\frac{r^2}{\epsilon^2}Q_p \log \frac{r^2}{\epsilon^2}Q_p$ if WGD or any sub-index of a disk selection heuristic is used.

Proof: The time complexities of the calculations for the availabilities of all task-PRF pairs ($O(N_t N_{\text{PRF}})$), the merge of the schedule (Q_d), and the preprocessing for the grid disks in Proposition 8 are common for the three different data structures. In the algorithm for SDBF, the data structures for the task selection are required for each disk rather than each PRF. For the brute force search, the time complexity of the task deletion is Q_d and the complexity of a call of **BI** from **HIED** is $N_{\text{intlv}}|K_d|_{\max}$ (refer to Proposition 3 and Lemma 1). For the multiple sorted task lists, the time complexity for the preprocessing is $O(Q_d \log |K_d|_{\max} N_{\text{intlv}}^2)$, which dominates the complexities of other operations, such as the task deletion ($O(Q_d N_{\text{intlv}}^2)$) and the calls of **BI** ($O(N_t N_{\text{intlv}}^2)$) (refer to Lemma 2). For the orthogonal range trees, the time complexity for the preprocessing, the task deletion, and the calls of **BI** are $O(Q_d(\log |K_d|_{\max} + \log^2 N_{\text{intlv}}))$, $O(Q_d \log^2 N_{\text{intlv}})$, and $O(N_t N_{\text{intlv}} \log^2 N_{\text{intlv}})$, respectively (refer to Lemma 3). Then the lemma is concluded by Proposition 8. ■

As in Theorem 1, the time complexities in Lemma 4 can be simplified with constant parameters N_{PRF} , N_{intlv} , r , and ϵ and a scalable number of targets.

Theorem 2. The time complexity of the pulse interleaving algorithm for SDBF using multiple sorted task lists or orthogonal range trees is $O(N_t^2 \log N_t)$ if N_{PRF} , N_{intlv} , r , and ϵ are constant.

Proof: Since $|K_p|_{\max} \leq N_t$, $|K_d|_{\max} \leq N_t$, and $N_d = O(\frac{r^2}{\epsilon^2}Q_p)$, if N_{PRF} , N_{intlv} , r , and ϵ are constant, then $O(Q_p) \leq O(N_t N_{\text{PRF}}) = O(N_t)$, $O(Q_d) \leq O(N_t N_d) = O(N_t Q_p) = O(N_t^2)$, and the complexities in Lemma 4 are reduced to $O(N_t^2 \log N_t)$. ■

VI. CONCLUSIONS

This paper has formulated the pulse interleaving problem using multiple simultaneous received beams (MSRB) for multiple target tracking in a pulse Doppler phased array radar (PAR) by an integer program. The problem formulation is valid for both element and subarray level digital beamforming (DBF) architectures and heuristic pulse interleaving algorithms are presented for the problems of the different DBF levels. The complexity analysis show that the heuristic pulse interleaving algorithms can be executed in a practical computation time.

ACKNOWLEDGMENT

This work was supported by Basic Science Research Program through the National Research Foundation of Korea (NRF) funded by the Ministry of Science, ICT and Future Planning (2013008693)

REFERENCES

- [1] A. Farina and P. Neri, "Multitarget interleaved tracking for phased-array radar," *IEE Proceedings F Communications, Radar and Signal Processing*, vol. 127, no. 4, pp. 312–318, 1980.
- [2] A. J. Orman, C. N. Potts, A. K. Shahani, and A. R. Moore, "Scheduling for a multifunction phased array radar system," *European Journal of Operational Research*, vol. 90, no. 1, pp. 13–25, April 1996.
- [3] C.-S. Shih, S. Gopalakrishnan, P. Ganti, M. Caccamo, and L. Sha, "Template-based real-time dwell scheduling with energy constraint," in *Proc. 9th IEEE Real-Time and Embedded Technology and Applications Symp*, 2003, pp. 19–27.
- [4] C.-G. Lee, P.-S. Kang, C.-S. Shih, and L. Sha, "Schedulability envelope for real-time radar dwell scheduling," *IEEE Transactions on Computers*, vol. 55, no. 12, pp. 1599–1613, 2006.
- [5] S. Ghosh, R. Rajkumar, J. Hansen, and J. Lehoczky, "Integrated QoS-aware resource management and scheduling with multi-resource constraints," *Real-Time Systems*, vol. 33, no. 1-3, pp. 7–46, 2006.
- [6] M. Elshafei, H. D. Sherali, and J. C. Smith, "Radar pulse interleaving for multi-target tracking," *Naval Research Logistics*, vol. 51, no. 1, pp. 72–94, 2004.
- [7] T. Cheng, Z. He, and T. Tang, "Novel radar dwell scheduling algorithm based on pulse interleaving," *Journal of Systems Engineering and Electronics*, vol. 20, no. 2, pp. 247–253, 2009.
- [8] J. N. Gupta, "Comparative evaluation of heuristic algorithms for the single machine scheduling problem with two operations per job and time-lags," *Journal of Global Optimization*, vol. 9, no. 3-4, pp. 239–253, 1996.
- [9] A. Orman and C. Potts, "On the complexity of coupled-task scheduling," *Discrete Applied Mathematics*, vol. 72, no. 1-2, pp. 141–154, 1997.
- [10] A. A. Ageev and A. E. Baburin, "Approximation algorithms for UET scheduling problems with exact delays," *Operations Research Letters*, vol. 35, no. 4, pp. 533–540, 2007.
- [11] M. Skolnik, *Radar Handbook*, ser. Electronics electrical engineering. McGraw-Hill, 2007.
- [12] A. Moore, D. Salter, and W. Stafford, "MESAR (multi-function, electronically scanned, adaptive radar)," in *(RADAR 97) International Radar Conference*, 1997, pp. 55–59.
- [13] H. Deng, B. Himed, and M. Wicks, "Concurrent extraction of target range and doppler information by using orthogonal coding waveforms," *Signal Processing, IEEE Transactions on*, vol. 55, no. 7, pp. 3294–3301, 2007.
- [14] M. Skolnik, *Introduction to Radar Systems*. McGraw-Hill, 2001.

- [15] S. A. Hovanessian, "Medium PRF performance analysis," *IEEE Transactions on Aerospace and Electronic Systems*, vol. AES-18, no. 3, pp. 286–296, 1982.
- [16] D. Wiley, S. Parry, C. Alabaster, and E. Hughes, "Performance comparison of PRF schedules for medium PRF radar," *IEEE Transactions on Aerospace and Electronic Systems*, vol. 42, no. 2, pp. 601–611, 2006.
- [17] I. Long, W. H. and K. A. Harriger, "Medium PRF for the AN/APG-66 radar," *Proceedings of the IEEE*, vol. 73, no. 2, pp. 301–311, 1985.
- [18] M. A. Richards, J. A. Scheer, and W. A. Holm, *Principles of Modern Radar: Basic Principles*. SciTech Publishing, 2010.
- [19] W. L. Melvin and J. A. Scheer, *Principles of Modern Radar: Advanced Techniques*. SciTech Publishing, 2012.
- [20] W. V. Aulock, "Properties of phased arrays," *Proceedings of the IRE*, vol. 48, no. 10, pp. 1715–1727, 1960.
- [21] D. S. Hochbaum and W. Maass, "Approximation schemes for covering and packing problems in image processing and VLSI," *J. ACM*, vol. 32, no. 1, pp. 130–136, Jan 1985.
- [22] G. K. Das, R. Fraser, A. Loopez-Ortiz, and B. G. Nickerson, "On the discrete unit disk cover problem," *International Journal of Computational Geometry & Applications*, vol. 22, no. 05, pp. 407–419, 2012.
- [23] B. Chazelle and D. Lee, "On a circle placement problem," *Computing*, vol. 36, no. 1-2, pp. 1–16, 1986.
- [24] K. L. Clarkson and K. Varadarajan, "Improved approximation algorithms for geometric set cover," *Discrete & Computational Geometry*, vol. 37, no. 1, pp. 43–58, 2007.
- [25] C. Liao and S. Hu, "Polynomial time approximation schemes for minimum disk cover problems," *Journal of Combinatorial Optimization*, vol. 20, no. 4, pp. 399–412, 2010.
- [26] N. Mustafa and S. Ray, "Improved results on geometric hitting set problems," *Discrete & Computational Geometry*, vol. 44, no. 4, pp. 883–895, 2010.
- [27] M. R. Korupolu, C. Plaxton, and R. Rajaraman, "Analysis of a local search heuristic for facility location problems," *Journal of Algorithms*, vol. 37, no. 1, pp. 146–188, 2000.
- [28] A. W. Neebe and M. R. Rao, "An algorithm for the fixed-charge assigning users to sources problem," *The Journal of the Operational Research Society*, vol. 34, no. 11, pp. 1107–1113, 1983.
- [29] K. Holmberg, M. Ronnqvist, and D. Yuan, "An exact algorithm for the capacitated facility location problems with single sourcing," *European Journal of Operational Research*, vol. 113, no. 3, pp. 544–559, 1999.
- [30] R. Sridharan, "A lagrangian heuristic for the capacitated plant location problem with single source constraints," *European Journal of Operational Research*, vol. 66, no. 3, pp. 305–312, 1993.
- [31] M. Ronnqvist, S. Tragantalermsak, and J. Holt, "A repeated matching heuristic for the single-source capacitated facility location problem," *European Journal of Operational Research*, vol. 116, no. 1, pp. 51–68, 1999.
- [32] R. K. Ahuja, J. B. Orlin, S. Pallottino, M. P. Scaparra, and M. G. Scutella, "A multi-exchange heuristic for the single-source capacitated facility location problem," *Management Science*, vol. 50, no. 6, pp. 749–760, 2004.
- [33] D. S. Hochbaum, "Heuristics for the fixed cost median problem," *Mathematical Programming*, vol. 22, pp. 148–162, 1982.